

# Stepwise Laser Photolysis Studies of $\beta$ -Bond Cleavage in Highly Excited Triplet States of Biphenyl Derivatives Having C–O Bonds

Minoru Yamaji,\* Akiko Kojima, and Seiji Tobita

Department of Chemistry, Gunma University, Kiryu 376-8515, Japan

Received: September 5, 2006; In Final Form: November 22, 2006

Photochemical profiles of  $\beta$ -bond dissociation in highly excited triplet states ( $T_n$ ) of biphenyl derivatives having C–O bonds were investigated in solution, using stepwise laser photolysis techniques. The lowest triplet states ( $T_1$ ) were produced by triplet sensitization of acetone (Ac) upon 308-nm laser photolysis. The molar absorption coefficients of the  $T_1$  states were determined using triplet sensitization techniques. Any photochemical reactions were absent in the  $T_1$  states. Upon 355-nm laser flash photolysis of the  $T_1$  states, they underwent fragmentation, because of homolysis of the C–O bond in the  $T_n$  states from the observations of the transient absorption of the corresponding radicals. The quantum yields ( $\Phi_{\text{dec}}$ ) for the decomposition of the  $T_1$  states upon the second 355-nm laser excitation were determined. Based on the  $\Phi_{\text{dec}}$  values and the bond dissociation energies (BDEs) for the C–O bond fission, the state energies ( $E_{\text{RT}}$ ) of the reactive highly excited triplet states ( $T_{\text{R}}$ ) were determined. It was revealed that (i) the  $\Phi_{\text{dec}}$  was related to the energy difference ( $\Delta E$ ) between the BDE and the  $E_{\text{RT}}$ , and (ii) the rate ( $k_{\text{dis}}$ ) of  $\beta$ -cleavage in the  $T_{\text{R}}$  state was formulated as being simply proportional to  $\Delta E$ . The reaction mechanism for  $\beta$ -bond cleavage in the  $T_{\text{R}}$  states was discussed.

## Introduction

Photoinduced bond dissociation is one of the well-known reactions in photochemistry and photobiology. As with photolytic bond cleavage of aromatic carbonyl compounds, Norrish Type I and II reactions, and carbon–heteroatom dissociation that occurs at the  $\alpha$ - and  $\beta$ -positions of the carbonyl have been widely studied by means of product analysis and time-resolved transient measurements.<sup>1–28</sup> A new-type bond cleavage ( $\omega$ -cleavage) of carbonyl compounds has been recently studied from the view point of the spin multiplicity and electronic configurations of the dissociative states.<sup>29</sup> On the other hand, photoinduced homolytic and heterolytic  $\beta$ -cleavage of the benzylic carbon–heteroatom  $\sigma$  bond is also well-documented to understand the mechanism and the nature of the relationship among the substituent groups, the excited-state energy, and the spin multiplicity of the reactive states.<sup>30</sup> The bond dissociation energy (BDE) is one of the useful parameters to qualify the stability of the chemical bonds against the dissociation in excited states of aromatic compounds. Generally, the chemical bond can be ready to be cleaved if only the excited-state energy of the reactive state is higher than the BDE. In our earlier work, we have investigated  $\beta$ -cleavage of C–X bonds (where X = Br, Cl, OH, and SH) of triplet biphenyl derivatives by means of laser flash triplet sensitization.<sup>31</sup> The  $\beta$ -cleavage of the C–S bond was observed, whereas that of the C–O bond was absent. In fact, the BDE of the C–S bond in *p*-phenylbenzyl mercaptan (56 kcal/mol) was smaller than the triplet energy (64 kcal/mol), whereas that of the C–O bond in biphenyl methanol (78 kcal/mol) is larger than the triplet energy.<sup>31</sup> Conversely, the C–O bond may be cleavable if the pertinent compound has other dissociative excited states that are higher in energy than the lowest triplet ( $T_1$ ) state. The formation of the higher triplet state can be readily achieved, using the second laser photolysis of

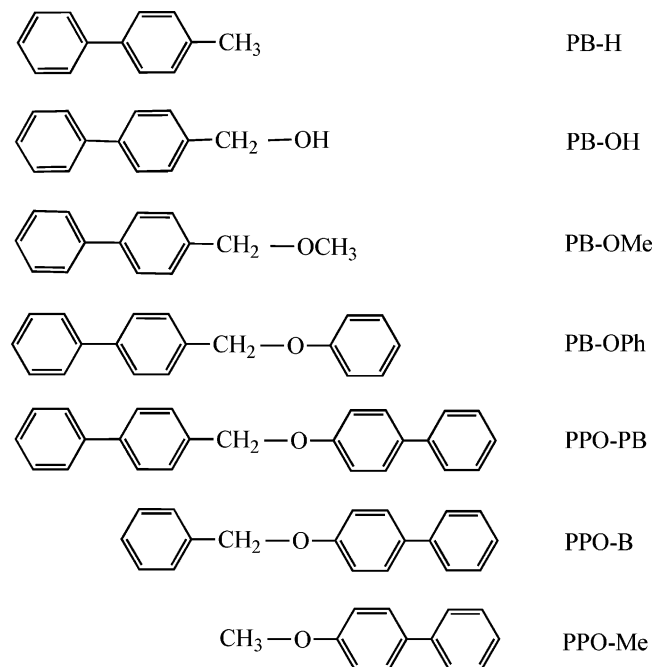
the  $T_1$  state. This method of multistep excitation has been widely used to study photophysical and photochemical processes in highly excited states.<sup>32–40</sup> Recently, two-color two-laser photolysis techniques have been applied to observe the C–O bond dissociation in highly excited triplet ( $T_n$ ) states of aromatic carbonyl compounds ( $\omega$ -cleavage) and naphthylmethyl derivatives ( $\beta$ -cleavage), and to determine the quantum yields of fragmentation in the highly excited triplet states.<sup>41</sup> However, systematic investigations are lacking, such as determination of the actual excited-state energy or formulation of the dissociation yields or the rates, as a function of the BDE.

Therefore, in the present work, we systematically investigate the C–O bond cleavage that occurs at the benzylic position of two types of biphenyl derivatives—*p*-phenylbenzyl derivatives (PB–X) and *p*-phenylphenoxy derivatives (PPO–X)—by means of sequential excitation of 308- and 355-nm laser pulsing. The first 308-nm laser photolysis was performed to efficiently create the  $T_1$  states via the triplet sensitization of acetone (Ac). Upon the second 355-nm laser pulsing, the  $T_1$  state was further excited to the higher triplet states. Based on the dissociation yields, we determined the excited-state energies of the reactive  $T_n$  state, and we formulated the rate and the yield of the  $\beta$ -cleavage in the  $T_n$  state.

## Experimental Section

*p*-Phenyl toluene (PB–H), *p*-phenylbenzyl alcohol (PB–OH) and *p*-phenyl anisol (PPO–Me) were purchased commercially, and each was purified via repeated recrystallizations from hexane. *a*-Methoxy-4-phenyl toluene (PB–OMe) was synthesized according to the literature.<sup>42</sup> PB–OMe was purified by passage through a silica-gel column with benzene as the eluent. *a*-Phenoxy-4-phenyl toluene (PB–OPh),  $\alpha$ -(*p*-phenylbenzyl)-4-phenyl phenol (PPO–PB), and  $\alpha$ -benzyl-4-phenyl phenol (PPO–B) were synthesized via a reaction of 4-bromomethyl biphenyl or  $\alpha$ -bromotoluene with phenol or *p*-phenyl phenol in

\* Author to whom correspondence should be addressed. Tel: +81-277-301212. Fax: +81-277-301212. E-mail: yamaji@chem.gunma-u.ac.jp.



PB = *p*-Phenylbenzyl, PPO = *p*-Phenylphenoxy, B = Benzyl

Ac, in the presence of potassium carbonate ( $K_2CO_3$ ). The products were purified via repeated recrystallizations from hexane. Acetonitrile (ACN), methanol, and ethanol were distilled for purification. ACN was used as the solvent, whereas a mixture of methanol and ethanol (1:1 v/v) was used as a matrix at 77 K. Absorption and emission spectra were recorded on a JASCO model U-best 50 spectrophotometer and a Hitachi model F-4010 fluorescence spectrophotometer, respectively. All the samples for transient absorption measurements were prepared in darkness and degassed in a quartz cell with a path length of 1 cm, using several freeze–pump–thaw cycles on a high vacuum line. Transient absorption measurements were performed at 295 K, unless noted, or in the temperature range between  $-22$  °C and  $57$  °C. The temperature of the sample in a quartz dewar was maintained with hot water ( $>295$  K) or with a mixture of methanol and liquid nitrogen ( $<295$  K) within a precision of  $\pm 0.5$  °C during the measurement. A XeCl excimer laser (wavelength of  $\lambda = 308$  nm; Lambda Physik, model Lextra 50) was used as the first excitation light source, whereas the third (355-nm) harmonics of a Nd<sup>3+</sup>:YAG laser (JK Lasers, model HY-500; pulse width = 8 ns) was used as the second excitation light source. The details of the detection system for the time profiles of the transient absorption have been reported elsewhere.<sup>43</sup> The incidence direction of the second 355-nm laser beam was parallel to that of the first 308-nm laser light. The transient data obtained by laser flash photolysis were analyzed using the least-squares best-fitting method. The transient absorption spectra were taken with a Unisoku model USP-554 system, which can provide a transient absorption spectrum with one laser pulse.

## Results and Discussion

**Absorption and Emission Measurements.** Figure 1 shows the absorption and fluorescence spectra of the employed compounds in ACN at 295 K and the phosphorescence spectra, in a glass matrix, of a mixture of methanol and ethanol (1:1 v/v) at 77 K.

It was confirmed that the excitation spectra for the emission agreed well with the corresponding absorption spectra. The

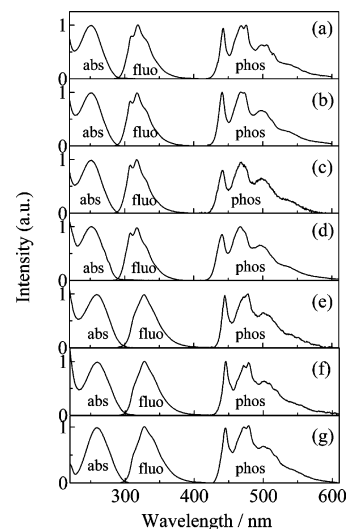


**Figure 1.** Absorption and fluorescence spectra in acetonitrile (ACN) at 295 K and phosphorescence spectra in a mixture of methanol and ethanol (1:1 v/v) at 77 K of (a) PB–H, (b) PB–OH, (c) PB–OMe, (d) PB–OPh, (e) PPO–PB, (f) PPO–B, and (g) PPO–Me.

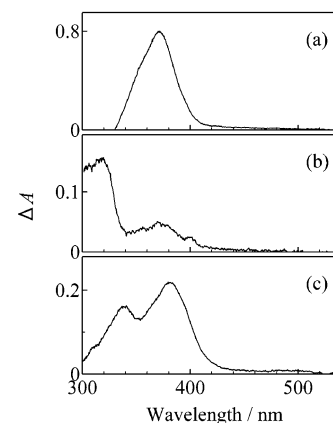


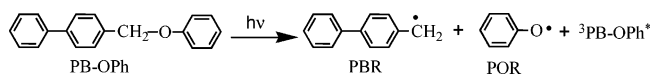
**Figure 2.** Transient absorption spectra at 500 ns obtained upon 266-nm laser pulsing in ACN solutions of (a) PB–H, (b) PB–OPh, and (c) PPO–B.

absorption and fluorescence spectra of PB–X (where X = H, OH, OMe, and OPh) are similar to each other, in regard to the shape and maximum wavelengths, but are different from those of PPO–X (where X = PB, B, and Me). The energy levels of the lowest triplet ( $T_1$ ) state were determined from the phosphorescence origins to be 65.0 kcal/mol for PB–X compounds and 64.2 kcal/mol for BPO–X compounds, whereas those of the lowest excited singlet states were 92.8 kcal/mol for PB–X compounds and 91.9 kcal/mol for BPO–X compounds. From the shape of the absorption and emission spectra, the compounds used can be clearly divided into two groups, from the viewpoint of the photophysical properties: *p*-phenylbenzyl derivatives (PB–X, where X = H, OH, OMe, and OPh) and *p*-phenylphenoxy derivatives (PPO–X, where X = PB, B, and Me).

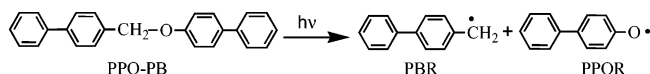
**Photochemical Profiles upon Direct Excitation.** To elucidate photochemical reactions upon direct excitation of the compounds used, 266-nm laser photolysis was performed. Figure 2 shows typical transient absorption spectra at 500 ns after 266-nm laser pulsing in the ACN solutions of the compounds that were used.

The transient absorption spectrum at 370 nm obtained for PB–H (Figure 2a) is ascribable to that of triplet PB–H.<sup>31</sup> The transient absorption spectra obtained for PB–OH, PB–OMe, and PPO–Me were similar to triplet PB–H in the shape and

the wavelength of the transient absorption band. These observations for PB–H, PB–OH, PB–OMe, and PPO–Me indicate that any appreciable photochemical reactions are absent in these excited singlet states, resulting in the efficient formation of the triplet states via intersystem crossing. With PB–OPh, the absorption bands at 320 and 400 nm in Figure 2b are observed, along with the triplet absorption band at 370 nm. The former can be ascribable to the absorption band of the *p*-phenylbenzyl radical (PBR), with an absorption coefficient of  $20\,000\text{ dm}^3\text{ mol}^{-1}\text{ cm}^{-1}$  at 320 nm,<sup>31</sup> whereas the latter is due to the phenoxy radical (POR) with an absorption coefficient of  $2000\text{ dm}^3\text{ mol}^{-1}\text{ cm}^{-1}$  at 400 nm.<sup>44</sup> From the observations of the triplet state and these radicals, it is indicative that the C–O bond cleavage occurs in the excited singlet states competitively with intersystem crossing to the triplet state.



The similar  $\beta$ -bond dissociation in PPO–B can be recognized from the transient absorption spectrum (Figure 2c) having an absorption band at 340 nm, which must be due to the *p*-phenylphenoxy radical (PPOR), with an absorption coefficient of  $21\,300\text{ dm}^3\text{ mol}^{-1}\text{ cm}^{-1}$  at 340 nm<sup>46</sup> and an absorption band at 310 nm that is due to the benzyl radical.<sup>48</sup> The absorption band at 380 nm is the triplet–triplet absorption of PPO–B. The photochemical profiles of PPO–B seem to resemble those of PB–OPh. With PPO–PB, the absorption bands of PBR at 320 nm and PPOR at 340 nm can be observed without an appreciable triplet absorption at  $\sim 380$  nm. The absence of the triplet absorption in the transient absorption spectrum for PPO–PB indicates that (i) the deactivation of the excited singlet states is governed by  $\beta$ -bond fission and fluorescent emission, and (ii) the intersystem crossing is inefficient.



After the depletion of the triplet absorptions, any new absorption bands did not appear. This demonstrates that any photochemical reactions do not occur in the lowest triplet states ( $T_1$ ) of the compounds that have been used.

We tried to determine the radical yields by quenching the triplets with the dissolved oxygen. However, as the number of the laser pulses increased, new transient absorption bands increasingly appeared in the wavelength region of 350–430 nm, presumably because of triplet benzaldehyde derivatives that were produced from the reaction of the benzyl radical derivatives with the dissolved oxygen. Therefore, we were unable to determine the yield after direct 266-nm laser photolysis.

**Triplet Sensitization Using Triplet Acetone.** To produce triplet states of the used compounds efficiently, we performed triplet sensitization, using acetone (Ac) as a triplet energy donor upon 308-nm laser photolysis. Because of the fact that the triplet energy of Ac is larger (74.0 kcal/mol)<sup>49</sup> than those of the used compounds (64–65 kcal/mol), triplet energy transfer can occur. Figure 3 shows a time profile of absorbance at 370 nm obtained after 308-nm laser pulsing in an Ac( $0.6\text{ mol dm}^{-3}$ )/PB–OPh( $1.7 \times 10^{-3}\text{ mol dm}^{-3}$ ) system.

The intensity of the absorbance increases with a first-order rate of  $2.7 \times 10^6\text{ s}^{-1}$ . A transient absorption spectrum obtained 1.0  $\mu\text{s}$  after laser pulsing (see inset in Figure 3) is undoubtedly due to triplet PB–OPh. Therefore, the growth of the absorption in Figure 3 is due to triplet energy transfer from triplet Ac to

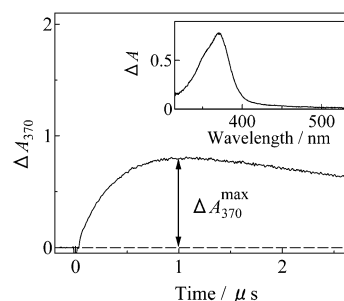


**Figure 3.** Time profile of absorbance at 370 nm obtained upon 266-nm laser pulsing in an Ac ( $0.6\text{ mol dm}^{-3}$ )/PB–OPh ( $1.7 \times 10^{-3}\text{ mol dm}^{-3}$ ) system in ACN. (Ac = acetone.) Inset shows a transient absorption spectrum obtained at 1.0  $\mu\text{s}$ .

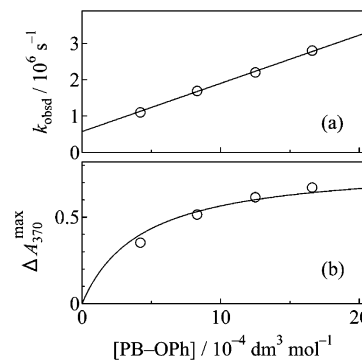


**Figure 4.** (a) Rate ( $k_{\text{obsd}}$ ) for the growth of triplet PB–OPh, plotted as a function of [PB–OPh] upon 308-nm laser photolysis in Ac ( $0.6\text{ mol dm}^{-3}$ )/PB–OPh systems in ACN. (b) Plots of the maximum absorbance at 370 nm ( $\Delta A_{370}^{\text{max}}$ ), as a function of [PB–OPh] obtained upon 308-nm laser photolysis in Ac ( $0.6\text{ mol dm}^{-3}$ )/PB–OPh systems in ACN. Solid curve was drawn using eq 2.

PB–OPh, resulting in the formation of triplet PB–OPh. The triplet absorption spectra of PB–X, as well as those of PPO–X, were similar to each other (see Supporting Information). These similarities indicate that the triplet exciton of PB–X and PPO–X is, respectively, localized on the *p*-phenylbenzyl (PB) and *p*-phenylphenoxy (PPO) moieties, irrespective of substituent X.

Figure 4a shows the rates ( $k_{\text{obsd}}$ ) of the growth of triplet PB–OPh, plotted as a function of the concentration of PB–OPh, [PB–OPh]. Because of the fact that the plots give a straight line, the parameter  $k_{\text{obsd}}$  can be formulated using eq 1:

$$k_{\text{obsd}} = k_0 + k_q[\text{PB-OPh}] \quad (1)$$

where  $k_0$  and  $k_q$ , respectively, represent the decay rate of triplet PB–OPh in the absence of PB–OPh and the rate constant for quenching of triplet Ac by PB–OPh. From the intercept and the slope of the line, the values of  $k_0$  and  $k_q$  were determined to be  $5.7 \times 10^5\text{ s}^{-1}$  and  $1.3 \times 10^9\text{ dm}^3\text{ mol}^{-1}\text{ s}^{-1}$ , respectively.

Figure 4b shows the maximum absorbance ( $\Delta A_{370}^{\text{max}}$ ) of triplet PB–OPh produced by triplet sensitization, plotted as a function of [PB–OPh]. As [PB–OPh] increases, the value of  $\Delta A_{370}^{\text{max}}$  increases, but not linearly. The  $\Delta A_{370}^{\text{max}}$  value of triplet PB–OPh produced via triplet sensitization can be formulated using eq 2:

$$\Delta A_{370}^{\text{max}} = k_q[\text{PB-OPh}]\alpha_{\text{TET}}^{\text{T-T}}\epsilon_{370}^{\text{Ac}}\Phi_{\text{ISC}}^{\text{Ac}}I_{\text{abs}}^{\text{Ac}}(k_0 + k_q[\text{PB-OPh}])^{-1} \quad (2)$$

where  $\alpha_{\text{TET}}^{\text{T-T}}$ ,  $\epsilon_{370}^{\text{Ac}}$ ,  $\Phi_{\text{ISC}}^{\text{Ac}}$ , and  $I_{\text{abs}}^{\text{Ac}}$  are the efficiency of triplet energy transfer from triplet Ac to PB–OPh, the molar absorption coefficient of triplet PB–OPh at 370 nm, the triplet yield of

**TABLE 1: Triplet Energy ( $E_T$ ), Molar Absorption Coefficient of Triplets ( $\epsilon^{T-T}$ ), Quenching Rate Constant ( $k_q$ ) of Triplet Acetone, Decomposition Yield ( $\Phi_{\text{dec}}$ ) of Triplets upon Second Laser Photolysis, Heats of Formation ( $\Delta_f H(\text{DP-LG})$  and  $\Delta_f H(\text{LG}\cdot)$ ) of the Parent Molecules and the Leaving Groups, and Bond Dissociation Energy (BDE) of the Compounds Used in the Present Work**

| compound (DP-LG) | $E_T^a$ (kcal/mol) | $\epsilon^{T-T}$ ( $\text{dm}^3 \text{mol}^{-1} \text{cm}^{-1}$ ) | $\lambda_{\text{max}}$ (nm) | $k_q$ ( $\times 10^9 \text{dm}^3 \text{mol}^{-1} \text{s}^{-1}$ ) | $\Phi_{\text{dec}}$ | $\Delta_f H(\text{DP-LG})$ (kcal/mol) | $\Delta_f H(\text{LG}\cdot)$ (kcal/mol) | BDE (C–O) <sup>b</sup> (kcal/mol) |
|------------------|--------------------|---|-----------------------------|---|---------------------|---------------------------------------|---|-----------------------------------|
| PB–H             | 65.0               | 28000   | 370                         | 1.1   | 0                   | 38.0                                  | 52.1                                    | 91.6 <sup>c</sup>                 |
| PB–OH            | 65.0               | 28000   | 370                         | 1.1   | 0.08                | 1.6                                   | 3.0                                     | 78.9                              |
| PB–OMe           | 65.0               | 27000   | 370                         | 1.2   | 0.17                | 5.3                                   | –6.8                                    | 65.4                              |
| PB–Oph           | 65.0               | 29000   | 370                         | 1.3   | 0.22                | 39.7                                  | 13.4                                    | 51.2                              |
| PPO–PB           | 64.2               | 27000 <sup>d</sup>  | 380                         | <i>e</i>  | 0.10                | 63.9                                  | 77.5                                    | 51.1                              |
| PPO–B            | 64.2               | 27000   | 380                         | 1.3   | 0.14                | 43.4                                  | 51.5                                    | 45.2                              |
| PPO–Me           | 64.2               | 27000   | 385                         | 1.4   | 0                   | 9.9                                   | 29.8                                    | 57.4                              |

<sup>a</sup> Determined from the 0–0 origin of the phosphorescence spectrum obtained in a mixture of methanol and ethanol (1:1 v/v) at 77 K. <sup>b</sup> Determined by eq 5 using the values of  $\Delta_f H(\text{PBR}) = 77.5 \text{ kcal/mol}$  and  $\Delta_f H(\text{PPOR}) = 37.5 \text{ kcal/mol}$ . <sup>c</sup> BDE for the  $\text{CH}_2\text{–H}$  bond. <sup>d</sup> Assumed to be the same as that for PPO–B. <sup>e</sup> Not determined, because of the low solubility of PPO–PB in ACN at room temperature.

Ac (1.0),<sup>49</sup> and the number of photon fluxes of an incident 308-nm laser pulse absorbed by PB–Oph, respectively. The value of the parameter  $I_{\text{abs}}$  was determined using the absorption of triplet benzophenone (BP) in ACN as an actinometer, which is expressed using eq 3:<sup>50</sup>

$$\Delta A_T^{\text{BP}} = \epsilon_T^{\text{BP}} \Phi_{\text{ISC}}^{\text{BP}} I_{\text{abs}}^{\text{BP}} \quad (3)$$

where  $\Delta A_T^{\text{BP}}$ ,  $\epsilon_T^{\text{BP}}$ , and  $\Phi_{\text{ISC}}^{\text{BP}}$  are the initial absorbance at 520 nm for the formation of triplet benzophenone obtained immediately after laser pulsing, the molar absorption coefficient of triplet BP at 520 nm in ACN ( $6500 \text{ dm}^3 \text{mol}^{-1} \text{cm}^{-1}$ ),<sup>51</sup> and triplet yield of BP (1.0),<sup>49</sup> respectively. Using eqs 1–3, and assuming the efficiency of  $\alpha_{\text{TET}}$  to be unity, the  $\epsilon_{370}^{T-T}$  value of triplet PB–Oph was determined to be  $29\,000 \pm 2000 \text{ dm}^3 \text{mol}^{-1} \text{cm}^{-1}$  at 370 nm. Using the same procedures, the quenching rate constants ( $k_q$ ) for triplet sensitization of Ac and the molar absorption coefficients  $\epsilon^{T-T}$  of the triplets of the compounds used in the present work were determined, and they are listed in Table 1. Upon triplet sensitization, no transient absorption spectra except triplets were observed. These observations confirm that photodecomposition of the triplets used is absent, even in the presence of the triplet sensitizer.<sup>52</sup>

**Photochemical Profiles of Triplets upon the Second Laser Photolysis.** Because the triplets of the compounds used in the present work are shown to have absorption at 355 nm, photochemical features upon the second 355-nm laser photolysis of the sensitized triplets were investigated. Figure 5 shows transient absorption spectra at 1.5  $\mu\text{s}$  upon 308-nm laser pulsing in an Ac( $0.6 \text{ mol dm}^{-3}$ )/PB–Oph( $1.7 \times 10^{-3} \text{ mol dm}^{-3}$ ) system in the absence and the presence of the second 355-nm laser pulsing 1.2  $\mu\text{s}$  after the first laser pulsing.

The transient absorption spectrum in the absence of the second laser pulse is due to the triplet state of PB–Oph produced by triplet sensitization. In the presence of the second laser pulse, the intensity of the absorption for the triplet at 370 nm decreases (see the upper inset in Figure 5), whereas a new absorption band at 320 nm that is due to PBR appears immediately after the second 355-nm laser pulsing. These changes in the transient absorption spectra obtained upon the second laser photolysis indicate that  $\beta$ -cleavage at the C–O bond occurs in a highly excited triplet state ( $T_n$ ) of PB–Oph. The appreciable absorption spectrum for POR as the counter radical of PBR, was not observed in the transient absorption, presumably because the molar absorption coefficient of POR ( $2000 \text{ dm}^3 \text{mol}^{-1} \text{cm}^{-1}$  at 400 nm)<sup>44</sup> is smaller than that of triplet PB–Oph ( $15000 \text{ dm}^3 \text{mol}^{-1} \text{cm}^{-1}$  at 400 nm).

A quantum yield ( $\Phi_{\text{dec}}$ ) for the decomposition of the  $T_1$  state of PB–Oph upon the second 355-nm laser pulsing was

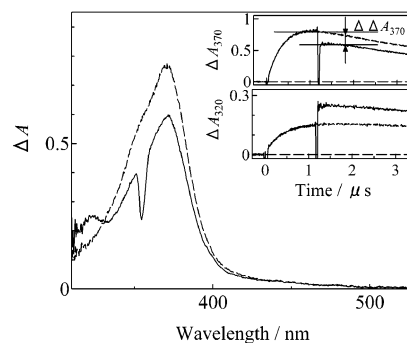


**Figure 5.** Transient absorption spectra obtained at 1.5  $\mu\text{s}$  upon 308-nm laser pulsing an Ac ( $0.6 \text{ mol dm}^{-3}$ )/PB–Oph ( $1.7 \times 10^{-3} \text{ mol dm}^{-3}$ ) system in ACN in the absence (dashed line) and the presence (solid line) of the second 355-nm laser pulsing at 1.2  $\mu\text{s}$ . The spike at 355 nm in the transient absorption spectrum in the red region of the wavelength spectrum is due to scattering of the second 355-nm laser pulse. Insets show time profiles at 370 nm (upper inset) and 320 nm (lower inset) in the absence (dashed line) and the presence (solid line) of the second 355-nm laser pulsing. The spikes at 1.2  $\mu\text{s}$  are due to scattering of the second 355-nm laser pulse.

determined using eq 4:

$$\Phi_{\text{dec}} = \Delta \Delta A_{370} I_0^{355} (1 - 10^{-\Delta A_{355}^{\text{TT}}}) \epsilon_{370}^{T-T-1} \quad (4)$$

where  $\Delta \Delta A_{370}$  represents an absorbance change at 370 nm for triplet PB–Oph due to decomposition after the second 355-nm laser photolysis,  $I_0^{355}$  is the intensity of the incident second 355-nm laser pulse, and  $\Delta A_{355}^{\text{TT}}$  is the absorbance of triplet BP–Oph at 355 nm, generated by triplet Ac sensitization. The quantity of  $I_0^{355}$  was determined using the triplet–triplet absorption of BP formed upon 355-nm laser photolysis in the ACN solution as an actinometer (see eq 3). The  $\Phi_{\text{dec}}$  value for triplet BP–Oph was determined to be  $0.22 \pm 0.02$ . Using the same procedures, definite  $\Phi_{\text{dec}}$  values for other compounds used in the present work were determined and are listed in Table 1. The transient absorption spectrum changes for the photodecomposition of other compounds after the second 355-nm laser photolysis can be observed in the Supporting Information. It was confirmed that all the  $\Phi_{\text{dec}}$  values were not influenced by the ambient temperatures from  $-22 \text{ }^\circ\text{C}$  to  $57 \text{ }^\circ\text{C}$ .

When homolytic cleavage proceeds in the triplet states of the employed diphenyl derivatives having leaving groups (DP-LG), triplet radical pairs of the diphenyl derivative radical (DP·; PBR or PPOR) and the leaving group radical (LG·) in the solvent cage  $^3(\text{DP}\cdot + \text{LG}\cdot)_{\text{cage}}$  initially formed, according to the spin-conservation rule. The triplet radical pair is free of geminate recombination, forming the parent molecule. Therefore, the

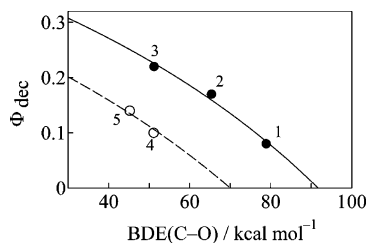


**Figure 6.** Quantum yields ( $\Phi_{\text{dec}}$ ) of triplet decomposition upon the second 355-nm laser pulsing in the triplets, plotted as a function of the bond dissociation energies (BDEs) for  $\text{CH}_2\text{-O}$ : 1, PB-OH; 2, PB-OMe; 3, PB-OPh; 4, PPO-PB; and 5, PPO-B. Solid and broken curves were calculated using eq 8.

obtained quantum yields ( $\Phi_{\text{dec}}$ ) can be regarded as those for the C-O bond cleavage in the higher triplet states of DP-LG. The residual quantum yields,  $1 - \Phi_{\text{dec}}$  are considered to be for the internal conversion from the  $T_n$  state to the  $T_1$  state ( $\Phi_{\text{ic}}$ ).

The bond dissociation energy (BDE) of the C-O  $\beta$ -bond in DP-LG was obtained using eq 5, based on the heats of formation ( $\Delta_f H$ ) for DP-LG, DP $\cdot$ , and LG $\cdot$ , computed using a semiempirical PM3 program contained in the MOPAC '97 software program.

$$\Delta_f H(\text{DP-LG}) = \Delta_f H(\text{DP}\cdot) + \Delta_f H(\text{LG}\cdot) - \text{BDE} \quad (5)$$

The  $\Delta_f H$  values used for DP $\cdot$  with the *p*-phenylbenzyl radical (PBR) and the *p*-phenylphenoxy radical (PPOR) were 77.5 and 37.5 kcal/mol, respectively, whereas those obtained for LG $\cdot$  (with H $\cdot$ , HO $\cdot$ , MeO $\cdot$ , PhO $\cdot$ , PhCH $_2\cdot$ , and CH $_3\cdot$ ) are listed in Table 1, along with the estimated BDE values.

Figure 6 shows plots of  $\Phi_{\text{dec}}$  as a function of the BDE for the C-O bonding thus obtained previously. A definite correlation between  $\Phi_{\text{dec}}$  and BDE is observed for PB-X and PPO-X.

The  $\Phi_{\text{dec}}$  value decreases as the BDE value for PB-X or PPO-X increases. From these two curves of the plots, it can be recognized that PPO-PB belongs to the PPO-X group, not to the PB-X compounds. Generally, for the occurrence of bond dissociation in excited states, the state energy must be larger than the BDE of the cleavable bond. Therefore, the intercept of the extrapolated line made by the plots of  $\Phi_{\text{dec}}$  may correspond to the state energy ( $E_{\text{RT}}$ ) of the highly excited triplet state ( $T_R$ ), which is reactive for  $\beta$ -cleavage. As with PPO-Me, the C-O bond dissociation was not observed when subjected to the second 355-nm laser photolysis, although the BDE (57.4 kcal/mol) for the C-O cleavage is definitely smaller than the triplet energy (64.2 kcal/mol). Currently, we have no ideas to rationalize this inactivity. The features of the plots in Figure 6 have been interpreted as follows.

Using the rates  $k_{\text{dis}}$  and  $k_{\text{ic}}$  of the  $\beta$ -cleavage and internal conversion from the  $T_R$  state to the  $T_1$  state, the quantum yield  $\Phi_{\text{dec}}$  is formulated using eq 6.

$$\Phi_{\text{dec}} = k_{\text{dis}}(k_{\text{dis}} + k_{\text{ic}})^{-1} \quad (6)$$

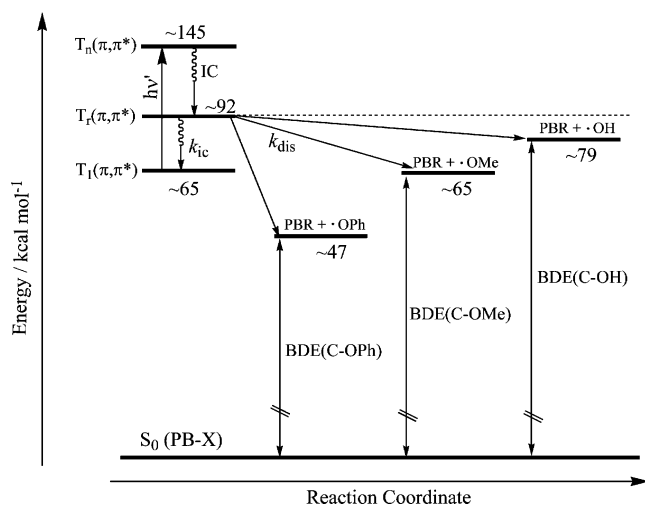
Here, we assume that the rate  $k_{\text{dis}}$  is simply proportional to the energy difference  $\Delta E$  between the  $E_{\text{RT}}$  and the BDE ( $\Delta E = E_{\text{RT}} - \text{BDE}$ ):

$$k_{\text{dis}} = \alpha \Delta E \quad (7)$$

Here,  $\alpha$  is a constant. The yield can be transformed using eq 7 and a constant,  $\beta$ :

$$\Phi_{\text{dec}} = \beta \Delta E (1 + \beta \Delta E)^{-1} \quad (8)$$

### SCHEME 1: Schematic Energy Diagram for Excited PB-X, Including the C-O Bond Dissociation Processes



where  $\beta = \alpha/k_{\text{ic}}$ . The solid line in Figure 6 was calculated using eq 8 and the best-fitted  $\beta$  and  $E_R$  values for PB-X ( $7.2 \times 10^{-3}$  mol/kcal and 91.7 kcal/mol, respectively). The plots follow the drawn curve well. This demonstrates that the rate or quantum yield of C-O  $\beta$ -bond cleavage in the highly excited triplet states of PB-X is controlled by the BDE value. The estimated  $E_{\text{RT}}$  value for PB-X is close to the  $S_1$  state energy ( $\sim 93$  kcal/mol) of PB-X. The BDE (91.6 kcal/mol) for the C-H bond of PB-H is similar to the estimated value of  $E_{\text{RT}}$ . The expression of eq 7 may be applicable only to the C-O bond cleavage in highly excited triplet states of PB-X. We examined this relationship using the  $\Phi_{\text{dec}}$  and BDE values of PPO-X. Because of the few PPO-X samples, we were unable to have best-fitted simulations for PPO-PB and PPO-B using eqs 7 and 8. Assuming that  $E_{\text{RT}} = 70$  kcal/mol for PPO-X, which is undoubtedly larger than the BDE values of PPO-B and PPO-PB, a  $\beta$  value of  $6.3 \times 10^{-3}$  mol/kcal was obtained by best-fitting. The broken line in Figure 6 was drawn using eq 8 and these values of  $\beta$  and  $E_R$  for PPO-X. As the BDE value decreases to zero,  $\Delta E$  increases close to the  $E_{\text{RT}}$  value. This approximation provides the ultimate  $\Phi_{\text{dec}}$  value ( $\Phi_{\text{dec}}^\infty$ ) for the present systems. Using eq 8 with the  $E_{\text{RT}}$  and  $\beta$  values, the  $\Phi_{\text{dec}}^\infty$  values obtained are 0.40 for PB-X and 0.31 for PPO-X. However, these values are not actual. After the BDE value is smaller than the energy level of the  $T_1$  state, the  $T_R$  state of the  $T_n$  states is not reactive anymore, but the  $T_1$  state would be alternatively.

Based on the obtained results, a schematic energy diagram for PB-X is depicted in Scheme 1, including the C-O bond cleavage processes.

After the  $T_1(\pi, \pi^*)$  state, where the triplet energy may be localized on the PB moiety, is excited to the  $T_n(\pi, \pi^*)$  state located at an energy level of 145 kcal/mol after 355-nm laser photolysis, the  $T_n$  state will be deactivated by internal conversion to the dissociative state,  $T_R(\pi, \pi^*)$ . Intersystem crossing from these highly excited triplets to the highly excited singlet states ( $S_n(\pi, \pi^*)$ ) can be negligible, because its rate should be substantially smaller than that of internal conversion, according to the spin-conservation rule. The energy level of the  $T_R(\pi, \pi^*)$  state for PB-X is located at  $\sim 92$  kcal/mol, from which the C-O  $\beta$ -cleavage proceeds with the dissociation rate ( $k_{\text{dis}}$ ), as a function of  $\Delta E$ , expressed by eq 7. It is originally suggested that the bond dissociation in excited states proceeds by avoided crossings between the reactive excited state with dissociative

potential surfaces of the same overall symmetry.<sup>54</sup> In that case, the electronic configuration of the dissociative potential for the C–O bond rupture studied in the present work is of the  $\sigma, \sigma^*$  type. Based on the fact that the  $\Phi_{\text{dec}}$  values were all independent of the ambient temperature in the range of  $-22$  °C to  $\sim 57$  °C, it is inferred that the  $T_{\text{R}}$  state strongly interacts with the dissociative  $^3(\sigma, \sigma^*)$  surface, which leads to free radicals without thermal activation energies. In turn, the absence of fragmentation in the  $T_1$  states can be interpreted by considering a large energy barrier for the interaction between the  $T_1(\pi, \pi^*)$  state and a dissociative triplet  $\sigma, \sigma^*$  potential.<sup>29d,40d,41b,c</sup> The energy diagram of PPO–X may be similar to that for PB–X. When the C–O bond dissociates in the  $T_{\text{R}}$  states of PB–X or PPO–X, a triplet  $\sigma$ -radical pair of PBR and  $\cdot X$ , or PPOR and  $\cdot X$ , may be initially produced in a solvent cage, according to the spin-conservation rule. The electronic configuration of the  $\sigma$ -radical in PBR or the benzyl radical may convert to that of the  $\pi$ -radical, because of the stabilization accrued from  $\pi$ -delocalization in PBR and the benzyl radical.

## Conclusion

By means of stepwise laser photolysis techniques, the C–O bond rupture of PB–X and PPO–X in the highly excited triplet states has been investigated. The photofragmentation of PB–A and PPO–X is absent in the  $T_1$  states. The quantum yield ( $\Phi_{\text{dec}}$ ) of the decomposition in the highly excited triplet states increases up to 0.24 for PB–X and 0.14 for PPO–X as the BDE of the C–O bond decreases, ranging from 79 kcal/mol to 45 kcal/mol. Based on the  $\Phi_{\text{dec}}$  values, the energy level ( $E_{\text{RT}}$ ) of the reactive state  $T_{\text{R}}$  for  $\beta$ -cleavage is estimated to be  $\sim 92$  kcal/mol for PB–X and  $\sim 70$  kcal/mol for PPO–X for the first time. The rate ( $k_{\text{dis}}$ ) for  $\beta$ -cleavage of PB–X and PPO–X in the  $T_{\text{R}}$  state is formulated as a function of  $\Delta E$  ( $\Delta E = E_{\text{RT}} - \text{BDE}$ ), as expressed by eq 7; that is, the  $k_{\text{dis}}$  value is simply proportional to the  $\Delta E$  value. The ultimate quantum yields ( $\Phi_{\text{dec}}^{\infty}$ ) are estimated to be 0.40 for PB–X and 0.31 for PPO–X. From the result that the  $\Phi_{\text{dec}}$  values are independent of the ambient temperature, the mechanism for the  $\beta$ -cleavage in the higher triplet states can be interpreted in terms of avoided crossing of the  $T_{\text{R}}$  state with a dissociative  $^3(\sigma, \sigma^*)$  potential surface.

**Supporting Information Available:** Transient absorption spectra of triplet PB–X and PPO–X obtained by acetone sensitization upon 308-nm laser photolysis and the transient absorption spectrum changes due to C–O bond dissociation of PB–OH, PB–OMe, PPO–PB, and PPO–B upon the second 355-nm laser photolysis (PDF). This material is available free of charge via the Internet at <http://pubs.acs.org>.

## References and Notes

- Turro, N. J. *Modern Molecular Photochemistry*; Benjamin/Cummings Publishing Co.: Menlo Park, CA, 1978.
- Gilbert, A.; Baggott, J. *Essentials of Molecular Photochemistry* (foreword by P. J. Wagner); Blackwell Scientific Publications: Oxford, U.K., 1991.
- Schönberg, A.; Fateen, A. K.; Omran, S. M. A. R. *J. Am. Chem. Soc.* **1956**, *78*, 1224.
- MacIntosh, C. L.; de Mayo, P.; Yip, R. W. *Tetrahedron Lett.* **1967**, 37.
- Collier, J. R.; Hill, J. *Chem. Commun.* **1968**, 700.
- (a) Shizuka, H. *Bull. Chem. Soc. Jpn.* **1968**, *41*, 2343. (b) Shizuka, H.; Tanaka, I. *Bull. Chem. Soc. Jpn.* **1969**, *42*, 52. (c) Shizuka, H.; Morita, T.; Mori, Y.; Tanaka, I. *Bull. Chem. Soc. Jpn.* **1969**, *42*, 1831.
- Whitten, D. G.; Punch, W. E. *Mol. Photochem.* **1970**, *2*, 77.
- Stermitz, F. R.; Nicodem, D. E.; Muralidharan, V. P.; O'Donnell, C. M. *Mol. Photochem.* **1970**, *2*, 87.
- Caserio, M. C.; Lauer, W.; Novinson, T. *J. Am. Chem. Soc.* **1970**, *92*, 6082.
- Majeti, S. *Tetrahedron Lett.* **1971**, 2523.
- (a) Wagner, P. *J. Acc. Chem. Res.* **1971**, *4*, 168. (b) Wagner, P. J.; Kelso, P. A.; Kempainen, A. E. *Mol. Photochem.* **1970**, *2*, 81. (c) Wagner, P. J.; Lindstrom, M. J. *J. Am. Chem. Soc.* **1987**, *109*, 3062.
- Heine, H.; Rosenkranz, J. J.; Rudolph, H. *Angew. Chem., Int. Ed. Engl.* **1972**, *11*, 974.
- Grunwell, J. R.; Marron, N. A.; Hanhan, S. *J. Org. Chem.* **1973**, *38*, 1559.
- Lewis, F. D.; Hoyle, C. H.; Magyar, J. G. *J. Org. Chem.* **1975**, *40*, 488.
- Brunton, G.; McBay, H. C.; Ingold, K. U. *J. Am. Chem. Soc.* **1977**, *99*, 4447.
- (a) Scaiano, J. C.; Perkins, M. J.; Sheppard, J. W.; Platz, M. S.; Barcus, R. L. *J. Photochem.* **1983**, *21*, 137. (b) Netto-Ferreira, J. C.; Leigh, W. L.; Scaiano, J. C. *J. Am. Chem. Soc.* **1985**, *107*, 2617. (c) McGimpsey, W. G.; Scaiano, J. C. *Can. J. Chem.* **1988**, *66*, 1474. (d) Scaiano, J. C.; Netto-Ferreira, J. C.; Wintgens, V. *J. Photochem. Photobiol. A: Chem.* **1991**, *59*, 265. (e) Boch, R.; Bohne, C.; Netto-Ferreira, J. C.; Scaiano, J. C. *Can. J. Chem.* **1991**, *69*, 2053. (f) Scaiano, J. C.; Netto-Ferreira, J. C. *J. Photochem.* **1986**, *32*, 253. (g) Netto-Ferreira, J. C.; Avellar, I. G. J.; Scaiano, J. C. *J. Org. Chem.* **1990**, *55*, 89.
- Fox, M. A.; Triebel, C. A. *J. Org. Chem.* **1983**, *48*, 835.
- Wismontski-Kinittel, T.; Kilp, T. *J. Phys. Chem.* **1984**, *88*, 110.
- Step, E. N.; Tarasov, V. F.; Buchachenko, A. L.; Turro, N. J. *J. Phys. Chem.* **1993**, *97*, 363.
- Leigh, W. J.; Banisch, J.-A. H.; Workentin, M. S. *J. Chem. Soc., Chem. Commun.* **1993**, 988.
- Hall, M.; Chen, L.; Pandit, C. R.; McGimpsey, W. G. *J. Photochem. Photobiol. A: Chem.* **1997**, *111*, 27.
- Kaneko, Y.; Hu, S.; Neckers, D. C. *J. Photochem. Photobiol. A: Chem.* **1998**, *114*, 173.
- Jockusch, S.; Landis, M. S.; Beat, F.; Turro, N. J. *Macromolecules* **2001**, *34*, 1619.
- (a) Suzuki, T.; Kaneko, Y.; Maeda, K.; Arai, T.; Akiyama, K.; Tero-Kubota, S. *Mol. Phys.* **2002**, *100*, 1469. (b) Suzuki, T.; Kaneko, Y.; Ikegami, M.; Arai, T. *Bull. Chem. Soc. Jpn.* **2004**, *77*, 801.
- (a) Allonas, X.; Lalevé, J.; Fouassier, J.-P. *J. Photochem. Photobiol. A: Chem.* **2003**, *159*, 127. (b) Allonas, X.; Lalevé, J.; Fouassier, J.-P. *J. Photopolym. Sci. Technol.* **2004**, *17*, 29.
- Cai, X.; Cygon, P.; Goldfuss, B.; Griesbeck, A. G.; Heckroth, H.; Fujitsuka, M.; Majima, T. *Chem.—Eur. J.* **2006**, *12*, 4662.
- Yamaji, M.; Wakabayashi, S.; Fukuda, K.; Inomata, S.; Tobita, S. *J. Photochem. Photobiol. A: Chem.* **2006**, *184*, 86.
- Yamaji, M.; Wakabayashi, S.; Tobita, S. *Res. Chem. Intermed.* **2006**, *32*, 749.
- (a) Yamaji, M.; Yoshihara, T.; Tachikawa, T.; Tero-Kubota, S.; Tobita, S.; Shizuka, H.; Marciniak, B. *J. Photochem. Photobiol. A: Chem.* **2004**, *162*, 513. (b) Yamaji, M.; Suzuki, A.; Ito, F.; Tero-Kubota, S.; Tobita, S.; Shizuka, H.; Marciniak, B. *J. Photochem. Photobiol. A: Chem.* **2005**, *170*, 253. (c) Yamaji, M.; Inomata, S.; Nakajima, S.; Akiyama, K.; Tobita, S.; Marciniak, B. *J. Phys. Chem. A* **2005**, *109*, 3843. (d) Yamaji, M.; Inomata, S.; Nakajima, S.; Akiyama, K.; Tero-Kubota, S.; Tobita, S.; Marciniak, B. *Chem. Phys. Lett.* **2006**, *417*, 211. (e) Yamaji, M.; Ogasawara, M.; Inomata, S.; Nakajima, S.; Tero-Kubota, S.; Tobita, S.; Marciniak, B. *J. Phys. Chem. A* **2006**, *110*, 10708.
- Fleming, S. A.; Pincock, J. A. *Mol. Supramol. Photochem.* **1999**, *3*, 211.
- Yamaji, M.; Kobayashi, J.; Tobita, S. *Photochem. Photobiol. Sci.* **2005**, *4*, 294.
- Yamamoto, S.; Kikuchi, K.; Kokubun, H. *Chem. Lett.* **1977**, 1173.
- Martin, M.; Bréhéret, E.; Tfibel, F.; Lacourbas, B. *J. Phys. Chem.* **1980**, *84*, 70.
- (a) McGimpsey, W. C.; Scaiano, J. C. *Chem. Phys. Lett.* **1987**, *138*, 13. (b) Wintgens, V.; Johnston, L. J.; Scaiano, J. C. *J. Am. Chem. Soc.* **1988**, *110*, 511. (c) McGimpsey, W. G.; Scaiano, J. C. *J. Am. Chem. Soc.* **1988**, *110*, 2299. (d) McGimpsey, W. G.; Scaiano, J. C. *J. Am. Chem. Soc.* **1989**, *111*, 335. (e) Redmond, R. W.; Scaiano, J. C.; Johnston, L. J. *J. Am. Chem. Soc.* **1990**, *112*, 398. (f) Bohne, C.; Kennedy, S. R.; Boch, R.; Negri, F.; Orlandi, G.; Siebrand, W.; Scaiano, J. C. *J. Phys. Chem.* **1991**, *95*, 10300.
- (a) Kajii, Y.; Suzuki, T.; Takatori, Y.; Shibuya, K.; Obi, K. *Bull. Chem. Soc. Jpn.* **1992**, *65*, 1349. (b) Takatori, Y.; Suzuki, T.; Kajii, Y.; Shibuya, K.; Obi, K. *Chem. Phys. Phys.* **1993**, *169*, 291.
- (a) Wang, Z.; Weininger, S. J.; McGimpsey, W. G. *J. Phys. Chem.* **1993**, *97*, 374. (b) Wang, Z.; McGimpsey, W. G. *J. Phys. Chem.* **1993**, *97*, 9668. (c) Gannon, T.; McGimpsey, W. G. *J. Org. Chem.* **1993**, *58*, 5639. (d) Smith, G. A.; McGimpsey, W. G. *J. Phys. Chem.* **1994**, *98*, 2923. (e) McGimpsey, W. G.; Samaniego, W. N.; Chen, L.; Wang, F. *J. Phys. Chem. A* **1998**, *102*, 8679.
- Adam, W.; Schneider, K.; Steeken, S. *J. Org. Chem.* **1997**, *62*, 3727.
- Akiyama, K.; Tero-Kubota, S.; Higuchi, J. *J. Am. Chem. Soc.* **1998**, *120*, 8269.

- (39) Miranda, M. A.; Pérez-Prieto, J.; Font-Sanchis, E.; Scaiano, J. C. *Acc. Chem. Res.* **2001**, *34*, 717.
- (40) (a) Cai, X.; Hara, M.; Kawai, K.; Tojo, S.; Majima, T. *Chem. Phys. Lett.* **2003**, *368*, 365; **2003**, *371*, 68; *Chem. Commun.* **2003**, 222; *Tetrahedron Lett.* **2003**, *44*, 6117. (b) Cai, X.; Sakamoto, M.; Hara, M.; Sugimoto, A.; Tojo, S.; Kawai, K.; Endo, M.; Fujitsuka, M.; Majima, T. *Photochem. Photobiol. Sci.* **2003**, *2*, 1209. (c) Cai, X.; Sakamoto, M.; Hara, M.; Tojo, S.; Kawai, K.; Endo, M.; Fujitsuka, M.; Majima, T. *J. Phys. Chem. A* **2004**, *108*, 7147; *Phys. Chem. Chem. Phys.* **2004**, *6*, 1735; *J. Phys. Chem. A* **2004**, *108*, 9361; *J. Phys. Chem. A* **2004**, *108*, 10941. (d) Cai, X.; Sakamoto, M.; Hara, M.; Inomata, S.; Yamaji, M.; Tojo, S.; Kawai, K.; Endo, M.; Fujitsuka, M.; Majima, T. *Chem. Phys. Lett.* **2005**, *407*, 402. (e) Sakamoto, M.; Cai, X.; Hara, M.; Fujitsuka, M.; Majima, T. *J. Phys. Chem. A* **2005**, *109*, 4657. (f) Cai, X.; Sakamoto, M.; Fujitsuka, M.; Majima, T. *Chem.—Eur. J.* **2005**, *11*, 6471. (g) Cai, X.; Tojo, S.; Fujitsuka, M.; Majima, T. *J. Phys. Chem. A* **2006**, *110*, 9319.
- (41) (a) Cai, X.; Sakamoto, M.; Hara, M.; Tojo, S.; Fujitsuka, M.; Ouchi, A.; Majima, T. *Chem. Commun.* **2003**, 3604; *J. Am. Chem. Soc.* **2004**, *126*, 7432. (b) Cai, X.; Sakamoto, M.; Yamaji, M.; Fujitsuka, M.; Majima, T. *J. Phys. Chem. A* **2005**, *109*, 5989. (c) Cai, X.; Sakamoto, M.; Hara, M.; Tojo, S.; Ouchi, A.; Sugimoto, A.; Kawai, K.; Endo, M.; Fujitsuka, M.; Majima, T. *J. Phys. Chem. A* **2005**, *109*, 3797. (d) Cai, X.; Sakamoto, M.; Yamaji, M.; Fujitsuka, M.; Majima, T. *Chem.—Eur. J.* in press.
- (42) Zimmerman, H. E.; Heydinger, J. A. *J. Org. Chem.* **1991**, *56*, 1747.
- (43) Yamaji, M.; Aihara, Y.; Itoh, T.; Tobita, S.; Shizuka, H. *J. Phys. Chem.* **1994**, *98*, 7014.
- (44) Amada, I.; Yamaji, M.; Sase, M.; Shizuka, H. *J. Chem. Faraday Trans.* **1995**, *91*, 2751.
- (45) Yamaji, M.; Wakabayashi, S.; Ueda, S.; Shizuka, H.; Tobita, S. *Chem. Phys. Lett.* **2003**, *368*, 41.
- (46) The  $\epsilon$  value of PPOR at 340 nm was determined based on that at 500 nm ( $2700 \text{ dm}^3 \text{ cm}^{-1} \text{ mol}^{-1}$ ).<sup>47</sup>
- (47) Yoshihara, T.; Yamaji, M.; Itoh, T.; Shizuka, H.; Shimokage, T.; Tero-Kubota, S. *Phys. Chem. Chem. Phys.* **2000**, *2*, 993.
- (48) Hiratsuka, H.; Okamoto, T.; Kuroda, S.; Okutsu, T.; Maeoka, H.; Taguchi, M.; Yoshinaga, T. *Res. Chem. Intermed.* **2001**, *27*, 137.
- (49) Montalti, M.; Credi, A.; Prodi, L.; Gandolfi, M. T. *Handbook of Photochemistry*, 3rd Edition (revised and expanded); CRC Press: Boca Raton, FL, 2006.
- (50) Yamaji, M.; Sekiguchi, T.; Hoshino, M.; Shizuka, H. *J. Phys. Chem.* **1992**, *96*, 9353.
- (51) Bensasson, R. V.; Gramain, J. C. *J. Chem. Soc., Faraday Trans.* **1980**, *76*, 1801.
- (52) We have reported that the C–S bond cleavage in the T<sub>1</sub> state of benzyl naphthyl sulfide is enhanced in the presence of a triplet sensitizer.<sup>53</sup>
- (53) Yamaji, M.; Ueda, S.; Shizuka, H.; Tobita, S. *Phys. Chem. Chem. Phys.* **2001**, *3*, 3102.
- (54) Dauben, W. G.; Salem, L.; Turro, N. J. *Acc. Chem. Res.* **1975**, *8*, 41.